Available online at www.sciencedirect.com
SCIENCE DIRECT®
Journal of Sound and Vibration 289 (2006) 130–147
JOURNAL OF SOUND AND VIBRATION
www.elsevier.com/locate/jsvi

Identification technique for nonlinear boundary conditions of a circular plate

Akihiro Suzuki[a,*], Keisuke Kamiya[a], Kimihiko Yasuda[b]

[a]*Department of Mechanical Science and Engineering, Nagoya University, Furo-cho, Chikusa-ku, Nagoya-shi, Aichi 4648603, Japan*
[b]*Department of Mechanical Engineering, Aichi Institute of Technology, 1247, Yachigusa, Yakusa-cho, Toyota-shi, Aichi 4700392, Japan*

Received 13 October 2003; received in revised form 20 January 2005; accepted 31 January 2005
Available online 12 July 2005

Abstract

As a basic study for developing an identification technique for boundary conditions of machines and structures, a new technique for a circular plate is proposed. This technique has features that do not require data measured on the boundary and is applicable to nonlinear boundary conditions. In the proposed technique, the boundary is modelled by springs and dampers as well as effective mass and moment of inertia. Then their characteristics are determined by using the analytical solution together with the experimental data. Since the technique is based on the analytical solution, it is applicable to any structure, provided that its analytical solution can be derived. Numerical simulation is conducted to show that the procedure determines the boundary conditions accurately.

1. Introduction

To analyse the dynamic behaviour of machines and structures, numerical methods such as finite element method are often used. Such numerical methods, however, do not always yield accurate results. One of the reasons for this is its difficulty to specify the actual boundary conditions accurately.

*Corresponding author. Tel.: +81 52 789 2782; fax: +81 52 789 5333.
E-mail address: akihiro@nuem.nagoya-u.ac.jp (A. Suzuki).

0022-460X/$ - see front matter © 2005 Elsevier Ltd. All rights reserved.
doi:10.1016/j.jsv.2005.01.058

Nomenclature

a	radius of the plate
A_{imn}, B_{imn}	unknown constants to express deflection in the form of analytical solutions
C	damping coefficient of the plate
E	Young's modulus of the plate
f	excitation
f_m	measured excitation
F_r	nonlinear restoring force of the boundary
F_d	nonlinear damping force of the boundary
F_n, F_n^*	nth order Fourier coefficients in time of the excitation
$F_{cmn}, F_{smn}, \ldots$	mth order Fourier coefficients in the circumferential direction ϕ of F_n, F_n^*
$\bar{F}_{cmn}, \bar{F}_{smn}, \ldots$	Hankel transform of $F_{cmn}, F_{smn}, \ldots$
$G_{cmn}, G_{smn}, \ldots$	parts of deflection, particular solutions
h	thickness of the plate
I	effective moment of inertia of the boundary
J_m	the Bessel function of the first kind of order m
$k_w, \alpha_w, \ldots$	functions as coefficients of restoring force in the form of the polynomial
$k_{wm}, \alpha_{wm}, \ldots$	Fourier coefficients in the circumferential direction of $k_w, \alpha_w, \ldots$
l_1	truncation order of Fourier series in time
l_2	truncation order of Fourier series in the circumferential direction
l_3	truncation order of Fourier series in the circumferential direction
M_r	nonlinear restoring moment of the boundary
M_d	nonlinear damping moment of the boundary
(r, ϕ)	polar coordinates for the plate
u_{imn}, v_{imn}	real and imaginary parts of $\mathrm{J}_m(\lambda_{imr})$
w_m	measured deflection
w	deflection
W_n, W_n^*	nth order Fourier coefficients in time of deflection, homogeneous solutions
$W_{cmn}, W_{smn}, \ldots$	mth order Fourier coefficients in the circumferential direction ϕ of W_n, W_n^*
$\bar{W}_{cmn}, \bar{W}_{smn}, \ldots$	Hankel transform of $W_{cmn}, w_{smn}, \ldots$
θ	inclination in the radial direction
μ	effective mass of the boundary
ν	Poisson's ratio of the plate
ρ	density of the plate

As a means to grasp the characteristics of boundaries, experimental identification techniques have attracted interests of engineers, and many techniques have been proposed. Among them are techniques by Zhao et al. [1], Ren and Beards [2,3], Ahmadian et al. [4], Pabst and Hagedorn [5], Xiang et al. [6], Takahashi [7] and Sanayei et al. [8], and Zhu and Huang [9]. All these techniques, however, have a restriction that they can be applied only to the case in which boundary conditions are linear. In practical cases, the boundary conditions often become nonlinear due to clearance, friction, material properties and so on. Thus, techniques applicable to nonlinear boundary conditions are desired. Sato et al. [10] proposed an identification technique for nonlinear boundary conditions. This technique, however, requires data measured on the boundaries. There are many cases in which measurement of data on the boundaries is difficult.

In previous papers [11–15], with the aim of developing an identification technique which is applicable to nonlinear boundary conditions and does not require data measured on the boundaries, the authors proposed techniques for one-dimensional structures. In this paper, as a

continuation to the previous study, a technique applicable to two-dimensional structure is developed. Here a circular plate is considered.

In the first part of this paper, as a preparation, analytical solution for a circular plate with nonlinear boundary conditions is derived. Then an identification technique is proposed. In the technique, the boundary is modelled by springs and dampers. Depending on the case, effective mass and moment of inertia of the boundary are included in the model. Then their characteristics are determined by using the analytical solution together with the experimental data. Since the technique is based on the analytical solution, it is applicable to any structure, provided that its analytical solution can be derived. Finally, numerical simulation is conducted to discuss the applicability of the technique. In the simulation, responses of a circular plate are obtained from the equations of motion numerically, and random numbers are added to them as noise. With these data being regarded as experimental, identification of the boundary conditions is performed. In this way, it is shown that the proposed technique yields accurate results.

2. Proposition of an identification technique

2.1. Formulation of the problem

A problem of identification of nonlinear boundary conditions for a linear circular plate is considered. Dynamic properties of the plate, except the boundary conditions are assumed to be known. In practice, it is often difficult to apply excitation to, or to measure responses on the boundaries. So, in developing a technique, it is imposed that the excitation to and measurement on the boundary are not required.

To formulate the problem, the boundary is modelled, as shown in Fig. 1, by springs and dampers. The restoring force and moment produced by the springs are denoted by F_r and M_r, and the damping force and moment produced by the dampers are denoted by F_d and M_d. They can be nonlinear functions of deflection w and inclination θ or their velocities at the boundary. In some cases, effective mass μ and moment of inertia I of the boundary should be considered. In this case, these quantities are included in the model. In the following, for generality, μ and I are included. Under the above assumptions, the problem of identification of boundary conditions is reduced to

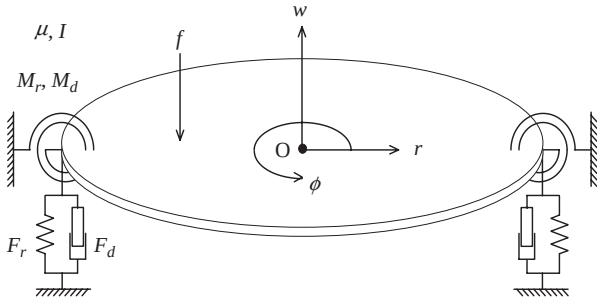

Fig. 1. Model of a circular plate.

the problem of determining F_r, M_r, F_d, M_d, μ and I by use of the experimental data of responses of the plate except for the boundary.

2.2. Derivation of the analytical solution

As a preparation for developing the identification procedure, the analytical solution of the circular plate is derived.

A circular plate with radius a, thickness h, density ρ, Young's modulus E and Poisson's ratio v is considered. At the boundary, the plate is supported as shown in Fig. 1. For this plate, the origin O is chosen at the centre of the circular plate, and the polar coordinate system $O-r\phi$ is introduced. The plate is supposed to be subjected to an excitation f and viscous damping force with damping coefficient C. Then the equation of motion of the plate is given by

$$D\nabla^4 w + C\frac{\partial w}{\partial t} + \rho h\frac{\partial^2 w}{\partial t^2} = f, \tag{1}$$

where

$$\nabla^2 = \frac{\partial^2}{\partial r^2} + \frac{\partial}{r\partial r} + \frac{\partial^2}{r^2\partial\phi^2}, \quad D = \frac{Eh^3}{12(1-v^2)}. \tag{2}$$

The boundary conditions at $r = a$ are given by

$$\begin{aligned} D\left[\frac{\partial}{\partial r}(\nabla^2 w) + \frac{1-v}{r}\frac{\partial}{\partial r}\left(\frac{\partial^2 w}{r\partial\phi^2}\right)\right] &= F_r + F_d + \mu\frac{\partial^2 w}{\partial t^2}, \\ D\left[\frac{\partial\theta}{\partial r} + v\left(\frac{\theta}{r} + \frac{\partial^2 w}{\partial\phi^2}\right)\right] &= -M_r - M_d - I\frac{\partial^2\theta}{\partial t^2}, \end{aligned} \tag{3}$$

where $\theta = \partial w/\partial r$.

Here, it is assumed that the excitation is a periodic function with fundamental angular frequency ω. Then f is expressed in the form of Fourier series in time t as follows:

$$f = \sum_{n=0}^{\infty} F_n(r,\phi)\cos n\omega t + \sum_{n=1}^{\infty} F_n^*(r,\phi)\sin n\omega t. \tag{4}$$

Since a circular plate is periodic in the circumferential direction with period 2π, $F_n(r,\phi)$ and $F_n^*(r,\phi)$ can be expressed in the form of Fourier series in angle ϕ as follows

$$\begin{aligned} F_n(r,\phi) &= \sum_{m=0}^{\infty} F_{cmn}(r)\cos m\phi + \sum_{m=1}^{\infty} F_{smn}(r)\sin m\phi, \\ F_n^*(r,\phi) &= \sum_{m=0}^{\infty} F_{cmn}^*(r)\cos m\phi + \sum_{m=1}^{\infty} F_{smn}^*(r)\sin m\phi. \end{aligned} \tag{5}$$

The quantities $F_{cmn}(r)$, $F_{smn}(r)$, $F_{cmn}^*(r)$ and $F_{smn}^*(r)$ are known when f is specified concretely.

Now the steady-state oscillation to the excitation is considered. Since the boundary conditions are nonlinear, various types of nonlinear oscillation may occur. Here, for simplicity, only a periodic oscillation whose period is the same as that of the excitation is considered. When other

types of oscillation such as sub-harmonic oscillation or combination resonance occur, one should express the solution in an appropriate form for the oscillation. Now the solution is assumed to be periodic, it can be expressed in the form of Fourier series in time as follows:

$$w = \sum_{n=0}^{\infty} W_n(r,\phi)\cos n\omega t + \sum_{n=1}^{\infty} W_n^*(r,\phi)\sin n\omega t, \tag{6}$$

where $W_n(r,\phi)$ and $W_n^*(r,\phi)$ are unknown functions. Similarly to Eq. (5), $W_n(r,\phi)$ and $W_n^*(r,\phi)$ in Eq. (6) can be expressed in the form of Fourier series in ϕ as follows

$$\begin{aligned} W_n(r,\phi) &= \sum_{m=0}^{\infty} W_{cmn}(r)\cos m\phi + \sum_{m=1}^{\infty} W_{smn}(r)\sin m\phi, \\ W_n^*(r,\phi) &= \sum_{m=0}^{\infty} W_{cmn}^*(r)\cos m\phi + \sum_{m=1}^{\infty} W_{smn}^*(r)\sin m\phi. \end{aligned} \tag{7}$$

In the above expressions, $W_{cmn}(r)$, $W_{smn}(r)$, $W_{cmn}^*(r)$ and $W_{smn}^*(r)$ are unknown functions of r. In order to determine $W_{cmn}(r)$, $W_{smn}(r)$, $W_{cmn}^*(r)$ and $W_{smn}^*(r)$, Eqs. (4)–(7) are substituted into Eq. (1), and in the resulting equations, coefficients of the terms $\cos n\omega t\cos m\phi$, $\cos n\omega t\sin m\phi$, $\sin n\omega t\cos m\phi$ and $\sin n\omega t\sin m\phi$ on both sides are equated. Then one obtains

$$\begin{aligned} \nabla_m^4 W_{cmn}(r) + \beta_n^4 W_{cmn}^*(r) - \alpha_n^4 W_{cmn}(r) &= \frac{F_{cmn}(r)}{D}, \\ \nabla_m^4 W_{smn}(r) + \beta_n^4 W_{smn}^*(r) - \alpha_n^4 W_{smn}(r) &= \frac{F_{smn}(r)}{D}, \\ \nabla_m^4 W_{cmn}^*(r) - \beta_n^4 W_{cmn}(r) - \alpha_n^4 W_{cmn}^*(r) &= \frac{F_{cmn}^*(r)}{D}, \\ \nabla_m^4 W_{smn}^*(r) - \beta_n^4 W_{smn}(r) - \alpha_n^4 W_{smn}^*(r) &= \frac{F_{smn}^*(r)}{D}, \end{aligned} \tag{8}$$

where

$$\nabla_m^2 = \frac{\mathrm{d}^2}{\mathrm{d}r^2} + \frac{\mathrm{d}}{r\mathrm{d}r} - \frac{m^2}{r^2}, \quad \alpha_n^4 = \frac{\rho h}{D}(n\omega)^2, \quad \beta_n^4 = \frac{C}{D}n\omega. \tag{9}$$

To obtain analytical solution of Eq. (8), first, the case for $n = 0$ is considered. Then Eq. (8) is reduced to

$$\nabla_m^4 W_{cm0}(r) = \frac{F_{cm0}(r)}{D}, \quad \nabla_m^4 W_{sm0}(r) = \frac{F_{sm0}(r)}{D}. \tag{10}$$

To solve Eq. (10), the homogeneous equations of Eq. (10) are considered. As shown in Ref. [16], the homogeneous solutions, not singular at $r = 0$, are given by

$$W_{cm0}(r) = B_{1m0}r^m + B_{2m0}r^{m+2}, \quad W_{sm0}(r) = B_{3m0}r^m + B_{4m0}r^{m+2}, \tag{11}$$

where B_{im0} $(i = 1,2,3,4)$ are arbitrary constants. The particular solutions of Eq. (10) are derived later together with those for $n \neq 0$.

Next, the case for $n \neq 0$ is considered. To solve Eq. (8), first, the homogeneous equations of Eq. (8) are considered. To obtain the homogeneous solutions, not singular at $r = 0$, the form of

the solution is assumed as

$$W_{cmn}(r) = A_{cmn}J_m(\lambda_n r), \quad W_{smn}(r) = A_{smn}J_m(\lambda_n r),$$
$$W^*_{cmn}(r) = A^*_{cmn}J_m(\lambda_n r), \quad W^*_{smn}(r) = A^*_{smn}J_m(\lambda_n r), \tag{12}$$

where J_m is the Bessel function of the first kind of order m, and A_{cmn}, A_{smn}, A^*_{cmn}, A^*_{smn} and λ_n are unknown constants. Substituting Eq. (12) into the homogeneous equations of Eq. (8) yields

$$\begin{aligned}
&(\lambda_n^4 - \alpha_n^4)A_{cmn}J_m(\lambda_n r) + \beta_n^4 A^*_{cmn}J_m(\lambda_n r) = 0,\\
&-\beta_n^4 A_{cmn}J_m(\lambda_n r) + (\lambda_n^4 - \alpha_n^4)A^*_{cmn}J_m(\lambda_n r) = 0,\\
&(\lambda_n^4 - \alpha_n^4)A_{smn}J_m(\lambda_n r) + \beta_n^4 A^*_{smn}J_m(\lambda_n r) = 0,\\
&-\beta_n^4 A_{smn}J_m(\lambda_n r) + (\lambda_n^4 - \alpha_n^4)A^*_{smn}J_m(\lambda_n r) = 0.
\end{aligned} \tag{13}$$

The condition for Eq. (13) to have non-zero A_{cmn}, A_{smn}, A^*_{cmn} and A^*_{smn} is given by

$$\begin{vmatrix} \lambda_n^4 - \alpha_n^4 & \beta_n^4 \\ -\beta_n^4 & \lambda_n^4 - \alpha_n^4 \end{vmatrix} = 0. \tag{14}$$

Solving Eq. (14) determines the constants λ_n. In the following, they are denoted as $\pm\lambda_{1n}$, $\pm\lambda_{2n}$, $\pm\lambda_{3n}$ and $\pm\lambda_{4n}$. For each λ_{in} $(i = 1, 2, 3, 4)$, the ratios of A^*_{cmn} to A_{cmn} and A^*_{smn} to A_{smn} are determined uniquely. Thus, the homogeneous solutions not singular at $r = 0$ are given as follows:

$$\begin{aligned}
W_{cmn}(r) &= A_{cmn1}J_m(\lambda_{1n}r) + A_{cmn2}J_m(\lambda_{2n}r) + A_{cmn3}J_m(\lambda_{3n}r) + A_{cmn4}J_m(\lambda_{4n}r),\\
W_{smn}(r) &= A_{smn1}J_m(\lambda_{1n}r) + A_{smn2}J_m(\lambda_{2n}r) + A_{smn3}J_m(\lambda_{3n}r) + A_{smn4}J_m(\lambda_{4n}r),\\
W^*_{cmn}(r) &= -\mathrm{j}A_{cmn1}J_m(\lambda_{1n}r) - \mathrm{j}A_{cmn2}J_m(\lambda_{2n}r) + \mathrm{j}A_{cmn3}J_m(\lambda_{3n}r) + \mathrm{j}A_{cmn4}J_m(\lambda_{4n}r),\\
W^*_{smn}(r) &= -\mathrm{j}A_{smn1}J_m(\lambda_{1n}r) - \mathrm{j}A_{smn2}J_m(\lambda_{2n}r) + \mathrm{j}A_{smn3}J_m(\lambda_{3n}r) + \mathrm{j}A_{smn4}J_m(\lambda_{4n}r),
\end{aligned} \tag{15}$$

where A_{cmni} and A_{smni} $(i = 1, 2, 3, 4)$ are arbitrary constants. In general, λ_{in} $(i = 1, 2, 3, 4)$ are complex, so are $J_m(\lambda_{in}r)$. In order to express the solution $W_{cmn}(r)$, $W_{smn}(r)$, $W^*_{cmn}(r)$ and $W^*_{smn}(r)$ in Eq. (15) in terms of real quantities, $J_m(\lambda_{in}r)$ are expressed in the form

$$J_m(\lambda_{1n}r) = u_{1mn}(r) + \mathrm{j}v_{1mn}(r), \quad J_m(\lambda_{2n}r) = u_{2mn}(r) - \mathrm{j}v_{2mn}(r),$$
$$J_m(\lambda_{3n}r) = u_{1mn}(r) - \mathrm{j}v_{1mn}(r), \quad J_m(\lambda_{4n}r) = u_{2mn}(r) + \mathrm{j}v_{2mn}(r). \tag{16}$$

Substituting Eq. (16) into Eq. (15) yields

$$\begin{aligned}
W_{cmn}(r) &= B_{1mn}u_{1mn}(r) + B_{2mn}v_{1mn}(r) + B_{3mn}u_{2mn}(r) + B_{4mn}v_{2mn}(r),\\
W_{smn}(r) &= B_{5mn}u_{1mn}(r) + B_{6mn}v_{1mn}(r) + B_{7mn}u_{2mn}(r) + B_{8mn}v_{2mn}(r),\\
W^*_{cmn}(r) &= -B_{2mn}u_{1mn}(r) + B_{1mn}v_{1mn}(r) + B_{4mn}u_{2mn}(r) - B_{3mn}v_{2mn}(r),\\
W^*_{smn}(r) &= -B_{6mn}u_{1mn}(r) + B_{5mn}v_{1mn}(r) + B_{8mn}u_{2mn}(r) - B_{7mn}v_{2mn}(r),
\end{aligned} \tag{17}$$

where B_{imn} $(i = 1, 2, \ldots, 8)$ are arbitrary constants.

Now the particular solutions of Eqs. (8) and (10) are considered. In order to obtain them, Hankel transform is used [17]. Applying the Hankel transform to Eq. (8), one has

$$
\begin{aligned}
(\xi^4-\alpha_n^4)\overline{W}_{cmn}(\xi)+\beta_n^4\overline{W}^*_{cmn}(\xi)&=\frac{\overline{F}_{cmn}(\xi)}{D},\\
(\xi^4-\alpha_n^4)\overline{W}_{smn}(\xi)+\beta_n^4\overline{W}^*_{smn}(\xi)&=\frac{\overline{F}_{smn}(\xi)}{D},\\
-\beta_n^4\overline{W}_{cmn}(\xi)+(\xi^4-\alpha_n^4)\overline{W}^*_{cmn}(\xi)&=\frac{\overline{F}^*_{cmn}(\xi)}{D},\\
-\beta_n^4\overline{W}_{smn}(\xi)+(\xi^4-\alpha_n^4)\overline{W}^*_{smn}(\xi)&=\frac{\overline{F}^*_{smn}(\xi)}{D},
\end{aligned}
\tag{18}
$$

where $\overline{W}_{cmn}(\xi), \overline{W}_{smn}(\xi), \ldots$ and $\overline{F}_{cmn}(\xi), \overline{F}_{smn}(\xi), \ldots$ are Hankel transform of $W_{cmn}(r), W_{smn}(r), \ldots$ and $F_{cmn}(r), F_{smn}(r), \ldots$. Solving Eq. (18) for $\overline{W}_{cmn}(\xi)$, $\overline{W}_{smn}(\xi)$, $\overline{W}^*_{cmn}(\xi)$ and $\overline{W}^*_{smn}(\xi)$, and performing the inverse Hankel transform yields the particular solutions of Eq. (8) as follows

$$
\begin{aligned}
G_{cmn}(r)&=\frac{1}{D}\int_0^\infty \frac{(\xi^4-\alpha_n^4)\overline{F}_{cmn}(\xi)-\beta_n^4\overline{F}^*_{cmn}(\xi)}{(\xi^4-\alpha_n^4)^2+\beta_n^8}\xi J_n(r\xi)\,\mathrm{d}\xi,\\
G_{smn}(r)&=\frac{1}{D}\int_0^\infty \frac{(\xi^4-\alpha_n^4)\overline{F}_{smn}(\xi)-\beta_n^4\overline{F}^*_{smn}(\xi)}{(\xi^4-\alpha_n^4)^2+\beta_n^8}\xi J_n(r\xi)\,\mathrm{d}\xi,\\
G^*_{cmn}(r)&=\frac{1}{D}\int_0^\infty \frac{\beta_n^4\overline{F}_{cmn}(\xi)+(\xi^4-\alpha_m^4)\overline{F}^*_{cmn}(\xi)}{(\xi^4-\alpha_m^4)^2+\beta_m^8}\xi J_n(r\xi)\,\mathrm{d}\xi,\\
G^*_{smn}(r)&=\frac{1}{D}\int_0^\infty \frac{\beta_n^4\overline{F}_{smn}(\xi)+(\xi^4-\alpha_n^4)\overline{F}^*_{smn}(\xi)}{(\xi^4-\alpha_n^4)^2+\beta_n^8}\xi J_n(r\xi)\,\mathrm{d}\xi,
\end{aligned}
\tag{19}
$$

where $G_{cmn}(r)$, $G_{smn}(r)$, $G^*_{cmn}(r)$ and $G^*_{smn}(r)$ are used instead of $W_{cmn}(r)$, $W_{smn}(r)$, $W^*_{cmn}(r)$ and $W^*_{smn}(r)$. Setting $n=0$ in Eq. (19) yields the particular solutions of Eq. (10).

Now the general solutions of Eqs. (8) and (10) are given. For $n=0$, combining Eqs. (11) and (19), one obtains

$$
\begin{aligned}
W_{cm0}(r)&=B_{1m0}r^m+B_{2m0}r^{m+2}+G_{cm0}(r),\\
W_{sm0}(r)&=B_{3m0}r^m+B_{4m0}r^{m+2}+G_{sm0}(r).
\end{aligned}
\tag{20}
$$

For $n\neq 0$, combining Eqs. (17) and (19), one obtains

$$
\begin{aligned}
W_{cmn}(r)&=B_{1mn}u_{1mn}(r)+B_{2mn}v_{1mn}(r)+B_{3mn}u_{2mn}(r)+B_{4mn}v_{2mn}(r)+G_{cmn}(r),\\
W_{smn}(r)&=B_{5mn}u_{1mn}(r)+B_{6mn}v_{1mn}(r)+B_{7mn}u_{2mn}(r)+B_{8mn}v_{2mn}(r)+G_{smn}(r),\\
W^*_{cmn}(r)&=-B_{2mn}u_{1mn}(r)+B_{1mn}v_{1mn}(r)+B_{4mn}u_{2mn}(r)-B_{3mn}v_{2mn}(r)+G^*_{cmn}(r),\\
W^*_{smn}(r)&=-B_{6mn}u_{1mn}(r)+B_{5mn}v_{1mn}(r)+B_{8mn}u_{2mn}(r)-B_{7mn}v_{2mn}(r)+G^*_{smn}(r).
\end{aligned}
\tag{21}
$$

In Eqs. (20) and (21), the coefficients B_{imn} $(i=1,2,\ldots,8)$ are determined by using the boundary conditions Eq. (3). Substituting Eqs. (20) and (21) into Eqs. (7),, (6) and (3) in this order and applying the harmonic balance procedure [18], one obtains the simultaneous nonlinear equations with respect to B_{imn}. Solving the resulting equations yields B_{imn}.

Now all of the unknown quantities have been obtained, the deflection w is determined in the form Eq. (6).

2.3. Proposition of an identification technique

Based on the analytical solution obtained in the previous section, an identification technique is developed.

The first step is to apply the periodic excitation of the form Eq. (4) and to measure the excitation and the steady-state deflection. The necessary number of the measurement points for deflection (r_i, ϕ_j) is discussed later. The number of the measurement points of the excitation are chosen so that the distribution of the excitation can be determined. When the distribution is known in advance, as in the case of a concentrated force, one point is enough for measurement of the excitation. In the following, such a case is considered.

The next step is to express the deflection in the analytical form for the purpose of obtaining the response at the boundary. The measured excitation f_m and deflection $w_m(r_i, \phi_j)$ are expressed, as Eqs. (4) and (6), in Fourier series in time domain of the form

$$\sum_{n=0}^{l_1} F_n \cos n\omega t + \sum_{n=1}^{l_1} F_n^* \sin n\omega t = f_m \tag{22}$$

and

$$\sum_{n=0}^{l_1} W_n(r_i, \phi_j) \cos n\omega t + \sum_{n=1}^{l_1} W_n^*(r_i, \phi_j) \sin n\omega t = w_m(r_i, \phi_j), \tag{23}$$

where l_1 denotes the truncation order. The coefficients in Eqs. (22) and (23) are determined, for example, by the fast Fourier transform algorithm. The determined Fourier coefficients in Eq. (22) and the knowledge of the distribution of the excitation yield the Hankel transform of F_{cmn}, F_{smn}, F_{cmn}^* and F_{smn}^* appeared in Eq. (19) in the previous section. Then, one can obtain the particular solutions $G_{cmn}(r_i)$, $G_{smn}(r_i)$, $G_{cmn}^*(r_i)$ and $G_{smn}^*(r_i)$ by Eq. (19). On the other hand, the Fourier coefficients $W_n(r_i, \phi_j)$ and $W_n^*(r_i, \phi_j)$ in Eq. (23) can be expressed by the Fourier series in angle ϕ of the form

$$\begin{aligned}
&\sum_{m=0}^{l_2} W_{cmn}(r_i) \cos m\phi_j + \sum_{m=1}^{l_2} W_{smn}(r_i) \sin m\phi_j = W_n(r_i, \phi_j),\\
&\sum_{m=0}^{l_2} W_{cmn}^*(r_i) \cos m\phi_j + \sum_{m=1}^{l_2} W_{smn}^*(r_i) \sin m\phi_j = W_n^*(r_i, \phi_j),
\end{aligned} \tag{24}$$

where l_2 denotes the truncation order. The number of the unknown quantities $W_{cmn}(r_i)$, $W_{smn}(r_i)$, $W_{cmn}^*(r_i)$ and $W_{smn}^*(r_i)$ for fixed n and r_i is $4l_2 + 2$. Since Eq. (24) contains two equations, choosing $2l_2 + 1$ or more measurement points in the circumferential direction, one can solve Eq. (24) for the unknown quantities by the least-squares method or by the fast Fourier transform algorithm.

The obtained particular solutions $G_{cmn}(r_i)$, $G_{smn}(r_i)$, $G_{cmn}^*(r_i)$ and $G_{smn}^*(r_i)$, and the Fourier coefficients $W_{cmn}(r_i)$, $W_{smn}(r_i)$, $W_{cmn}^*(r_i)$ and $W_{smn}^*(r_i)$ must satisfy the relationship Eqs. (20) and (21). Substituting them into Eqs. (20) and (21), one obtains sets of equations with respect to the

arbitrary constants B_{imn}. These equations are written as, for the case $n = 0$,

$$B_{1m0}r_i^m + B_{2m0}r_i^{m+2} = W_{cm0}(r_i) - G_{cm0}(r_i),$$
$$B_{3m0}r_i^m + B_{4m0}r_i^{m+2} = W_{sm0}(r_i) - G_{sm0}(r_i), \tag{25}$$

and for the case $n \neq 0$,

$$\begin{aligned}
&B_{1mn}u_{1mn}(r_i) + B_{2mn}v_{1mn}(r_i) + B_{3mn}u_{2mn}(r_i) + B_{4mn}v_{2mn}(r_i) = W_{cmn}(r_i) - G_{cmn}(r_i),\\
&B_{5mn}u_{1mn}(r_i) + B_{6mn}v_{1mn}(r_i) + B_{7mn}u_{2mn}(r_i) + B_{8mn}v_{2mn}(r_i) = W_{smn}(r_i) - G_{smn}(r_i),\\
&-B_{2mn}u_{1mn}(r_i) + B_{1mn}v_{1mn}(r_i) + B_{4mn}u_{2mn}(r_i) - B_{3mn}v_{2mn}(r_i) = W^*_{cmn}(r_i) - G^*_{cmn}(r_i),\\
&-B_{6mn}u_{1mn}(r_i) + B_{5mn}v_{1mn}(r_i) + B_{8mn}u_{2mn}(r_i) - B_{7mn}v_{2mn}(r_i) = W^*_{smn}(r_i) - G^*_{smn}(r_i).
\end{aligned} \tag{26}$$

The number of the unknown constants B_{imn} is 4 in Eq. (25) and 8 in Eq. (26) for a fixed n, while the number of equations is 2 in Eq. (25) and 4 in Eq. (26). Thus, choosing two or more measurement points in radial direction, one can solve Eqs. (25) and (26) for B_{imn} by the least-squares method.

In the above, data of deflection of the plate were used to determine B_{imn}. In some cases, it is possible to obtain data of inclination or strain of the plate in addition to those of deflection. In that case use of these data improves accuracy.

Now the constants B_{imn} and the particular solutions $G_{cmn}(r_i)$, $G_{smn}(r_i)$, $G^*_{cmn}(r_i)$ and $G^*_{smn}(r_i)$ have been determined, deflection w can be written as a function of t, r and ϕ in the form of Eq. (6). In this expression, setting $r = a$ gives the deflection at the boundary.

The final step of the identification procedure is to determine the characteristics of the unknown functions F_r, F_d, M_r, M_d, μ and I. As shown in Section 2.1, F_r and M_r are nonlinear functions of deflection w and inclination $\theta = \partial w/\partial r$, while F_d and M_d are nonlinear functions of their velocities $\dot{w}$ and $\dot{\theta}$. Hence in determining F_r, F_d, M_r and M_d, it is assumed that they are given by polynomials of the form

$$\begin{aligned}
F_r &= k_w(\phi)w + \alpha_w(\phi)w^2 + \beta_w(\phi)w^3 + \cdots,\\
F_d &= c_w(\phi)\dot{w} + \varsigma_w(\phi)\dot{w}^2 + \eta_w(\phi)\dot{w}^3 + \cdots,\\
M_r &= k_\theta(\phi)\theta + \alpha_\theta(\phi)\theta^2 + \beta_\theta(\phi)\theta^3 + \cdots,\\
M_d &= c_\theta(\phi)\dot{\theta} + \varsigma_\theta(\phi)\dot{\theta}^2 + \eta_\theta(\phi)\dot{\theta}^3 + \cdots,
\end{aligned} \tag{27}$$

where $k_w(\phi), \alpha_w(\phi), \ldots, k_\theta(\phi), \alpha_\theta(\phi), \ldots$ are unknown functions. Since these unknown functions as well as the effective mass $\mu = \mu(\phi)$ and moment of inertia $I = I(\phi)$ are periodic functions in ϕ with period 2π, they can be expressed in Fourier series:

$$k_w(\phi) = \sum_{m=0}^{l_3} k_{wm}\cos m\phi + \sum_{m=1}^{l_3} k^*_{wm}\sin m\phi,$$
$$\alpha_w(\phi) = \sum_{m=0}^{l_3} \alpha_{wm}\cos m\phi + \sum_{m=1}^{l_3} \alpha^*_{wm}\sin m\phi,$$
$$\vdots$$

$$\mu(\phi) = \sum_{m=0}^{l_3} \mu_m \cos m\phi + \sum_{m=1}^{l_3} \mu_m^* \sin m\phi,$$
$$I(\phi) = \sum_{m=0}^{l_3} I_m \cos m\phi + \sum_{m=1}^{l_3} I_m^* \sin m\phi, \tag{28}$$

where l_3 (usually $l_3 \leqslant l_2$) denotes the truncation order, and $k_{wm}, \alpha_{wm}, \ldots$ are unknown parameters. Thus the problem of identification is finally reduced to determination of these parameters.

To determine them, the deflection w on the boundary expressed in the form of Eq. (6) and Eqs. (27) and (28) are substituted into Eq. (3). Based on the harmonic balance procedure, the coefficients of terms $\cos n\omega t \cos m\phi$, $\cos n\omega t \sin m\phi$, $\sin n\omega t \cos m\phi$ and $\sin n\omega t \sin m\phi$ in both sides of the resulting equations are equated. Then simultaneous linear equations with respect to the unknown parameters are obtained:

$$[A]\{k_{w0} \quad \alpha_{w0} \quad \cdots \quad \mu_{l_3}^* \quad I_{l_3}^*\}^{\mathrm{T}} = \{b\}, \tag{29}$$

where $[A]$ is the matrix of coefficients of the unknown parameters and $\{b\}$ consists of the left-hand side of Eq. (3). Solving Eq. (29) by the least-squares method determines the unknown parameters. If necessary one can increase the number of Eq. (29) by changing the magnitude, frequency or position of the excitation and repeating the above steps. In general, it is expected that as the number of equations increases, the results become more accurate.

3. Numerical simulation

To show applicability of the proposed technique, numerical simulation is conducted. First, dynamic response is calculated by solving the equations of motion of a plate whose parameters are given appropriately. Then using the data thus obtained, identification is performed. Finally, the obtained results are compared to the original values of the parameters used for calculation of the response.

3.1. Calculation of the dynamic response

A circular plate whose material properties and dimensions are given in Table 1 is considered. Characteristics of the restoring force and moment at the boundary is supposed to be given by

$$F_r = k_w(\phi)w + \beta_w(\phi)w^3, \quad M_r = k_\theta(\phi)\theta + \beta_\theta(\phi)\theta^3,$$
$$F_d = c_w(\phi)\dot{w}, \quad M_d = c_\theta(\phi)\dot{\theta}, \tag{30}$$

where

$$c_w(\phi) = c_{w0}, \quad c_\theta(\phi) = c_{\theta 0},$$
$$k_w(\phi) = k_{w0} + k_{w1}^* \sin\phi, \quad k_\theta(\phi) = k_{\theta 0} + k_{\theta 1}^* \sin\phi,$$
$$\beta_w(\phi) = \beta_{w0} + \beta_{w1}^* \sin\phi, \quad \beta_\theta(\phi) = \beta_{\theta 0} + \beta_{\theta 1}^* \sin\phi. \tag{31}$$

Table 1
Material properties and dimensions of the circular plate

Radius	$a = 3.2 \times 10^{-1}$ m
Thickness	$h = 1.0 \times 10^{-3}$ m
Young's modulus	$E = 2.06 \times 10^{11}$ Pa
Density	$\rho = 7.84 \times 10^{3}$ kg/m^3
Damping	$C = 5.0 \times 10^{-1}$ Ns/m^3
Poisson's ratio	$v = 3.0 \times 10^{-1}$

Table 2
Parameters of the boundary

Parameters with respect to deflection			Parameters with respect to inclination		
μ_0	1.0×10^{-1}	(kg)	I_0	5.0×10^{-3}	(kgm^3)
μ_1	0.0	(kg)	I_1	0.0	(kgm^3)
μ_1^*	3.0×10^{-2}	(kg)	I_1^*	1.2×10^{-3}	(kgm^3)
c_{w0}	2.0	(Ns/m)	$c_{\theta 0}$	3.0	(Nms/rad^3)
c_{w1}	0.0	(Ns/m)	$c_{\theta 1}$	0.0	(Nms/rad^3)
c_{w1}^*	0.0	(Ns/m)	$c_{\theta 1}^*$	0.0	(Nms/rad^3)
k_{w0}	1.0×10^{4}	(N/m)	$k_{\theta 0}$	6.0×10^{2}	(Nm/rad)
k_{w1}	0.0	(N/m)	$k_{\theta 1}$	0.0	(Nm/rad)
k_{w1}^*	2.5×10^{3}	(N/m)	$k_{\theta 1}^*$	1.8×10^{2}	(Nm/rad)
α_{w0}	0.0	(N/m^2)	$\alpha_{\theta 0}$	0.0	(Nm/rad^2)
α_{w1}	0.0	(N/m^2)	$\alpha_{\theta 1}$	0.0	(Nm/rad^2)
α_{w1}^*	0.0	(N/m^2)	$\alpha_{\theta 1}^*$	0.0	(Nm/rad^2)
β_{w0}	4.5×10^{9}	(N/m^3)	$\beta_{\theta 0}$	6.0×10^{7}	(Nm/rad^3)
β_{w1}	0.0	(N/m^3)	$\beta_{\theta 1}$	0.0	(Nm/rad^3)
β_{w1}^*	1.5×10^{9}	(N/m^3)	$\beta_{\theta 1}^*$	1.8×10^{7}	(Nm/rad^3)

The effective mass $\mu(\phi)$ and moment of inertia $I(\phi)$ are also supposed to be given by

$$\mu(\phi) = \mu_0 + \mu_1^* \sin\phi, \quad I(\phi) = I_0 + I_1^* \sin\phi. \tag{32}$$

Values of the parameters in Eqs. (31) and (32) are shown in Table 2. Eqs. (31) and (32) imply that in this simulation a case is considered in which characteristics except the damping are almost uniform, but have fluctuations which are approximated by trigonometric functions in the circumferential direction.

As the excitation, concentrated harmonic force applied at point (r_f, ϕ_f)

$$f = \frac{F_{\text{ex}}}{r_f}\delta(r - r_f)\delta(\phi - \phi_f)\cos\omega t, \tag{33}$$

is considered. In Eq. (33), δ is Dirac's delta function, and values of the parameters are given as

$$F_{\text{ex}} = 0.8 \text{ [N]}, \quad r_f = 0.2 \text{ [m]}, \quad \phi_f = 3/2\pi.$$

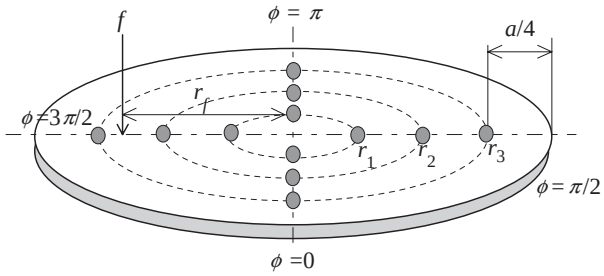

Fig. 2. Points of measurement and excitation.

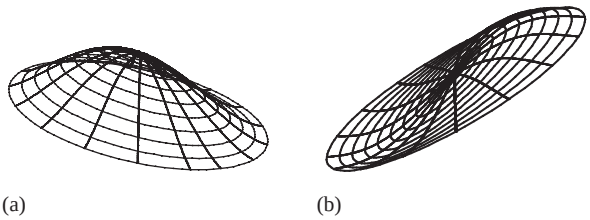

Fig. 3. (a) The first linear mode and (b) second linear mode of the plate.

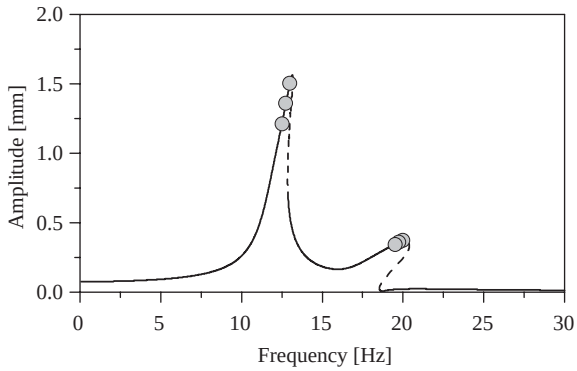

Fig. 4. Amplitude of fundamental frequency component at point $(r_1, 0)$: ——, stable; - - - - -, unstable; ○, frequencies for identification.

Twelve points shown in Fig. 2 are chosen as the measurement points. Response of the plate is obtained following the analysis procedure in Section 2.2. In Eq. (6), terms for $n = 1$ and 3 are retained since the excitation is harmonic and the nonlinearity is cubic. In Eq. (7), terms for $m = 0$ and 1 are retained since, as shown below, data in the resonance of the first and second modes are used for identification. For reference, the first and second linear modes of the plate are shown in Fig. 3. In this simulation, total of 24 unknown constants $B_{imn}\,(i = 1, 2, \ldots, 8)$ in Eq. (21) are

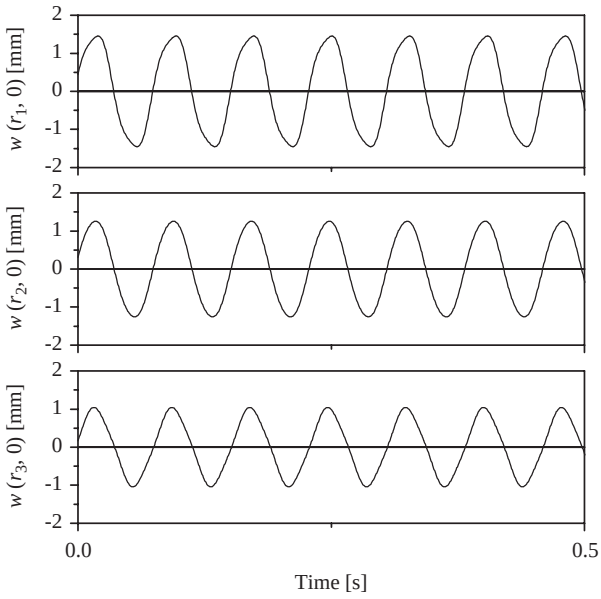

Fig. 5. Time histories of deflection at $(r_i, 0)$ $(i = 1, 2, 3)$ at 13 Hz.

derived by solving a set of simultaneous nonlinear equations. This set of equations was solved by the subroutine of Brent method [19]. Thus the deflection of the plate was obtained.

For identification data at six frequencies 12.50, 12.75, 13.00, 19.50, 19.75 and 20.00 Hz are used. These frequencies are near to the resonance frequencies of the first or second modes as shown in Fig. 4, which shows the resonance curve for the component of the fundamental frequency at the measurement point $(r_1, 0)$. Hence, data at these frequencies are expected to contain information about the boundary conditions including the nonlinearity. As examples of time histories of the deflection data at the measurement points $(r_i, 0)$ $(i = 1, 2, 3)$ at 13 Hz are shown in Fig. 5. In identification, these data were sampled at 1024 Hz, and 8192 points of data were used.

3.2. Application of the identification technique

3.2.1. Case in which data is not contaminated with noise

In this section, a case in which data are not contaminated with noise is considered. Following the identification procedure in Section 2.3, first, Fourier coefficients of Eqs. (22) and (23) are determined by the fast Fourier transform. Fig. 6 shows the Fourier spectrums of the data shown in Fig. 5. From Fig. 6, one can see that retaining in Eqs. (22) and (23) the terms from the first to the third order is enough.

Second, Fourier coefficients in Eq. (23) is expanded into Fourier series in angle ϕ, as the form of Eq. (24). Since data near to the resonance of the first and second modes are being used, the terms from the zeroth to the first order in Eq. (24) are retained. The coefficients in Eq. (24) are determined by the fast Fourier transform.

Third, the arbitrary constants B_{imn} in Eq. (26) are determined. In this case, for each frequency of the excitation, the number of B_{imn} becomes 36, while the number of equations of Eq. (26)

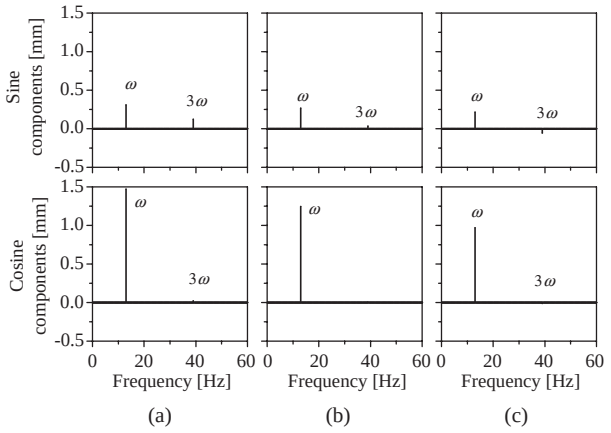

Fig. 6. Fourier spectrum of Fig. 5: (a) $(r_1, 0)$; (b) $(r_2, 0)$; (c) $(r_3, 0)$.

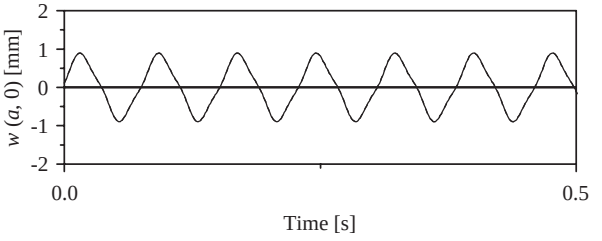

Fig. 7. Original and estimated time history of deflection at boundary $(a, 0)$ at 13 Hz: ——, original; - - - - -, estimated.

becomes 54 because 3 measurement points are chosen in the radial direction. So Eq. (26) can be solved by the least-squares method. Using the obtained B_{imn}, one can have the deflection at the boundary in the form of Eq. (6). As an example, time history of the deflection at the boundary for $\phi = 0$ at frequency 13 Hz is shown in Fig. 7 by dashed line. In the same figure, the deflection at the same point obtained from the equations of motion is plotted by solid line. It is seen that both data agree very well.

Fourth, the forms of the unknown functions F_r, F_d, M_r and M_d are assumed. Here they are assumed in the polynomials of the form

$$F_r = k_w(\phi)w + \alpha_w(\phi)w^2 + \beta_w(\phi)w^3, \quad M_r = k_\theta(\phi)\theta + \alpha_\theta(\phi)\theta^2 + \beta_\theta(\phi)\theta^3,$$
$$F_d = c_w(\phi)\dot{w}, \quad M_d = c_\theta(\phi)\dot{\theta}. \tag{34}$$

The coefficients of Eq. (34) are assumed in the Fourier series of the form

$$c_w(\phi) = c_{w0} + c_{w1}\cos\phi + c^*_{w1}\sin\phi, \quad c_\theta(\phi) = c_{\theta0} + c_{\theta1}\cos\phi + c^*_{\theta1}\sin\phi,$$
$$k_w(\phi) = k_{w0} + k_{w1}\cos\phi + k^*_{w1}\sin\phi, \quad k_\theta(\phi) = k_{\theta0} + k_{\theta1}\cos\phi + k^*_{\theta1}\sin\phi,$$
$$\alpha_w(\phi) = \alpha_{w0} + \alpha_{w1}\cos\phi + \alpha^*_{w1}\sin\phi, \quad \alpha_\theta(\phi) = \alpha_{\theta0} + \alpha_{\theta1}\cos\phi + \alpha^*_{\theta1}\sin\phi,$$
$$\beta_w(\phi) = \beta_{w0} + \beta_{w1}\cos\phi + \beta^*_{w1}\sin\phi, \quad \beta_\theta(\phi) = \beta_{\theta0} + \beta_{\theta1}\cos\phi + \beta^*_{\theta1}\sin\phi. \tag{35}$$

Table 3
Identified parameters without noise

Parameters	Original	Identified	Parameters	Original	Identified
μ_0	1.0×10^{-1}	1.000×10^{-1}	I_0	5.0×10^{-3}	5.000×10^{-3}
μ_1	0.0×10^{-1}	0.000×10^{-1}	I_1	0.0×10^{-3}	0.000×10^{-3}
μ_1^*	0.3×10^{-1}	0.300×10^{-1}	I_1^*	1.2×10^{-3}	1.200×10^{-3}
c_{w0}	2.0	2.000	$c_{\theta 0}$	3.0	3.000
c_{w1}	0.0	0.000	$c_{\theta 1}$	0.0	0.000
c_{w1}^*	0.0	0.000	$c_{\theta 1}^*$	0.0	0.000
k_{w0}	1.0×10^4	1.000×10^4	$k_{\theta 0}$	6.0×10^2	6.000×10^2
k_{w1}	0.0×10^4	0.000×10^4	$k_{\theta 1}$	0.0×10^2	0.000×10^2
k_{w1}^*	0.25×10^4	0.250×10^4	$k_{\theta 1}^*$	1.8×10^2	1.800×10^2
α_{w0}	0.0	0.000	$\alpha_{\theta 0}$	0.0	0.000
α_{w1}	0.0	0.000	$\alpha_{\theta 1}$	0.0	0.000
α_{w1}^*	0.0	0.000	$\alpha_{\theta 1}^*$	0.0	0.000
β_{w0}	4.5×10^9	4.500×10^9	$\beta_{\theta 0}$	6.0×10^7	6.000×10^7
β_{w1}	0.0×10^9	0.000×10^9	$\beta_{\theta 1}$	0.0×10^7	0.000×10^7
β_{w1}^*	1.5×10^9	1.500×10^9	$\beta_{\theta 1}^*$	1.8×10^7	1.800×10^7

Similarly, effective mass and moment of inertia are assumed in the Fourier series of the form

$$\mu(\phi) = \mu_0 + \mu_1 \cos\phi + \mu_1^* \sin\phi, \quad I(\phi) = I_0 + I_1 \cos\phi + I_1^* \sin\phi. \tag{36}$$

Finally, the unknown parameters are determined. Their number is 30, while the number of equations with respect to the unknown parameters is 36 for each frequency of the excitation. Since six frequencies have been chosen, the total number of the equations is 216. Thus the unknown parameters are determined by the least-squares method.

The determined parameters are shown in the column 'identified' in Table 3. In the same table, original values of the parameters are shown in the column 'original' for comparison. As seen in the table, the values of the determined parameters agree very well with those of the original parameters.

3.2.2. *Case in which data are contaminated with noise*

In this section, a case in which data are contaminated with noise is considered. Here, random numbers are added to the time histories as noise. In the following, the results are shown for the case in which the standard deviation of the random number is 2.5% of the average of the amplitudes at the measurement points. As an example, time histories obtained by adding random numbers to those in Fig. 5 are shown in Fig. 8 . Using these data, identification is performed. The conditions, such as the excitation or measurement points, and the assumptions, such as the form of the unknown functions Eqs. (34)–(36), for identification are the same as those in the previous sections.

The identified parameters are shown in the column 'identified' in Table 4. As seen in the table, the identified parameters except β_θ and I are acceptable, though the accuracy is worse than that in the previous case. To evaluate the accuracy of the identified results in terms of response, the

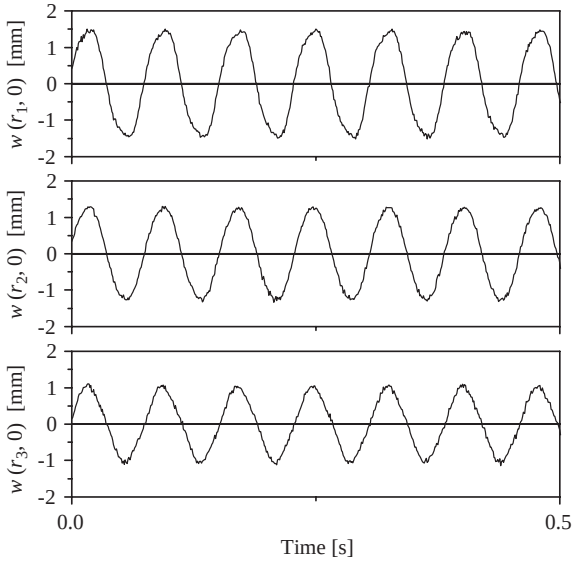

Fig. 8. Time histories of deflection added random numbers at $(r_i, 0)$ $(i = 1, 2, 3)$.

Table 4
Identified parameters with noise

Parameters	Original	Identified	Parameters	Original	Identified
μ_0	1.0×10^{-1}	0.960×10^{-1}	I_0	5.0×10^{-3}	4.561×10^{-3}
μ_1	0.0×10^{-1}	-0.022×10^{-1}	I_1	0.0×10^{-3}	-0.113×10^{-3}
μ_1^*	0.3×10^{-1}	0.298×10^{-1}	I_1^*	1.2×10^{-3}	1.196×10^{-3}
c_{w0}	2.0	2.039	$c_{\theta 0}$	3.0	2.951
c_{w1}	0.0	−0.016	$c_{\theta 1}$	0.0	−0.064
c_{w1}^*	0.0	−0.026	$c_{\theta 1}^*$	0.0	−0.037
k_{w0}	1.0×10^4	1.004×10^4	$k_{\theta 0}$	6.0×10^2	5.877×10^2
k_{w1}	0.0×10^4	0.002×10^4	$k_{\theta 1}$	0.0×10^2	-0.449×10^2
k_{w1}^*	0.25×10^4	0.249×10^4	$k_{\theta 1}^*$	1.8×10^2	1.644×10^2
α_{w0}	0.0×10^6	-0.017×10^6	$\alpha_{\theta 0}$	0.0×10^5	0.104×10^5
α_{w1}	0.0×10^6	0.017×10^6	$\alpha_{\theta 1}$	0.0×10^5	0.310×10^5
α_{w1}^*	0.0×10^6	0.022×10^6	$\alpha_{\theta 1}^*$	0.0×10^5	0.255×10^5
β_{w0}	4.5×10^9	4.412×10^9	$\beta_{\theta 0}$	6.0×10^7	6.523×10^7
β_{w1}	0.0×10^9	-0.064×10^9	$\beta_{\theta 1}$	0.0×10^7	4.316×10^7
β_{w1}^*	1.5×10^9	1.513×10^9	$\beta_{\theta 1}^*$	1.8×10^7	2.932×10^7

resonance curve is obtained using the identified parameters. The results are shown in Fig. 9. In this figure, solid and dashed lines indicate amplitude of stable and unstable response obtained from the original parameters, and circles indicate amplitude estimated from the identified parameters. The figure shows that in terms of response the identified parameters are accurate

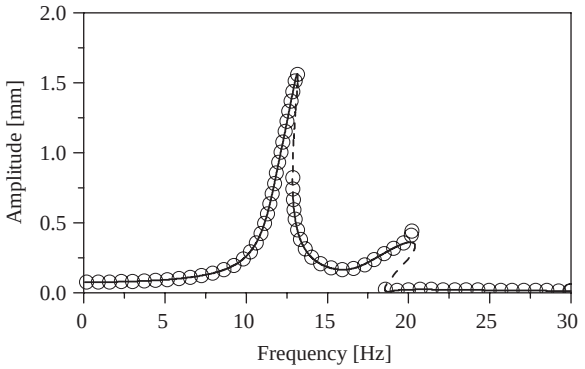

Fig. 9. Estimated resonance curve of fundamental frequency component at point $(r_1, 0)$: ——, original curve (stable); - - - - -, original curve (unstable); ◯, estimated amplitude by the identified parameters.

enough. This in turn implies that the parameters which do not have influence on the response are difficult to determine by the proposed technique.

4. Conclusions

As a basic study for developing an experimental identification technique applicable to nonlinear boundary conditions of a two-dimensional structure, a circular plate has been considered. A technique for it has been proposed. In the proposed technique, the boundary is modelled by springs, dampers, effective masses and moments of inertia. Their characteristics are determined by use of the data of steady-state deflection. By numerical simulation, it has been confirmed that the proposed technique determines the boundary conditions well.

Appendix

For a function $h(r)$, its Hankel transform of order m, $\bar{h}_m(\xi)$, is defined by

$$\bar{h}_m(\xi) = \int_0^\infty rh(r)J_m(\xi r)\,\mathrm{d}r.$$

Following the definition, it is shown that Hankel transform of the derivative $\nabla_m^2 h(r)$ is given by $-\xi^2\bar{h}(\xi)$.

References

[1] C.S. Zhao, M. Touratier, G. Coffinal, Identifications of dynamic characteristics of joints, *Proceedings of 4th IMAC*, Los Angeles, 1986, pp. 316–328.
[2] Y. Ren, C.F. Beards, An iterative FRF joints identification technique, *Proceedings of 11th IMAC*, Kissimmee, 1993, pp. 1133–1139.

[3] Y. Ren, C.F. Beards, Identification of 'effective' linear joints using coupling and joint identification techniques, *Journal of Vibration and Acoustics* 120 (1998) 331–338.
[4] H. Ahmadian, J.E. Mottershead, M.I. Friswell, Boundary condition identification by solving characteristics equations, *Journal of Sound and Vibration* 247 (2001) 755–763.
[5] U. Pabst, P. Hagedorn, Identification of boundary conditions as a part of model correction, *Journal of Sound and Vibration* 182 (1995) 565–575.
[6] J. Xiang, C. Zhou, X. Yuan, A new identification method for mechanical support properties from measured modal parameters, *Proceedings of 11th IMAC*, 1993, pp. 781–786.
[7] I. Takahashi, Identification for critical flutter load and boundary conditions of a beam using neural networks, *Journal of Sound and Vibration* 228 (1999) 857–870.
[8] M. Sanayei, J.A.S. McClain, S. Wadia-Fascetti, E.M. Santini, Parameter estimation incorporating modal data and boundary conditions, *Journal of Structural Engineering* 125 (1999) 1048–1055.
[9] J. Zhu, L. Huang, Estimation of boundary parameters of plate structures, *Journal of Sound and Vibration* 179 (1995) 455–461.
[10] H. Sato, Y. Iwata, S. Sugimoto, Identification of non-linear support systems by using transient response, *Journal of The Japan Society of Mechanical Engineers (Series C)* 61-585 (1995) 1906–1910 (in Japanese).
[11] K. Yasuda, Y. Goto, Experimental identification technique for boundary conditions of a beam (when boundary conditions are linear), *Journal of The Japan Society of Mechanical Engineers (Series C)* 60-570 (1994) 482–489 (in Japanese).
[12] Y. Goto, K. Yasuda, Experimental identification technique for boundary conditions of a beam (confirmation of applicability of the technique and its application to a rolling bearing), *Journal of The Japan Society of Mechanical Engineers (Series C)* 62-597 (1996) 1797–1804 (in Japanese).
[13] K. Yasuda, Y. Goto, Y. Hirose, Experimental identification technique for boundary conditions of a beam (when boundary conditions are non-linear), *Journal of The Japan Society of Mechanical Engineers (Series C)* 62-599 (1996) 2599–2605 (in Japanese).
[14] K. Yasuda, K. Kamiya, A. Suzuki, Experimental identification technique for boundary conditions of a circular plate (non-linear axisymmetrical problems), *Journal of The Japan Society of Mechanical Engineers (Series C)* 68-667 (2002) 747–753 (in Japanese).
[15] K. Yasuda, K. Kamiya, A. Suzuki, Experimental identification technique for non-linear boundary conditions of a beam, *Proceedings of Ninth Conference on Non-linear Vibrations, Stability, and Dynamics of Structures*, 2002, p. 55.
[16] S. Timoshenko, S. Woinowsky-Krieger, *Theory of Plates and Shells*, McGraw-Hill, New York, 1959.
[17] W. Nowacki, *Baudynamik*, Springer, New York, 1974.
[18] P. Hagedorn, *Non-linear Oscillations*, Clarendon Press, Oxford, 1981.
[19] Fujitsu Scientific Subroutine Library II user's manual, Fujitsu Ltd, 1987.